HHS Public Access

Author manuscript

Magn Reson Med. Author manuscript; available in PMC 2019 August 01.

Published in final edited form as:

Magn Reson Med. 2018 August ; 80(2): 529–537. doi:10.1002/mrm.27045.

Simultaneous Bilateral Knee MR Imaging

Feliks Kogan[1], **Evan G. Levine**[1,2], **Akshay S. Chaudhari**[1,3], **Uchechukwuka D. Monu**[1,2], **Kevin Epperson**[1], **Edwin H.G. Oei**[4], **Garry E. Gold**[1,3,5], and **Brian A. Hargreaves**[1,2,3]

[1]Department of Radiology, Stanford University, Stanford, California, USA [2]Department of Electrical Engineering, Stanford University, Stanford, California, USA [3]Department of Bioengineering, Stanford University, Stanford, California, USA [4]Department of Radiology & Nuclear Medicine, Erasmus MC, University Medical Center, Rotterdam, Netherlands [5]Department of Orthopaedic Surgery, Stanford University, Stanford, California, USA

Abstract

Purpose—To demonstrate and evaluate the scan time and quantitative accuracy of simultaneous bilateral knee imaging compared to single knee acquisitions

Methods—Hardware modifications and safety testing was performed to enable MR imaging with two 16-channel flexible coil-arrays. Noise covariance and SENSE g-factor maps for the dual-coil-array configuration were computed to evaluate coil cross-talk and noise amplification. Ten healthy volunteers were imaged on a 3T MRI with both dual-coil-array bilateral knee and single-coil-array single knee configurations. Two experienced musculoskeletal radiologists compared relative image quality between blinded image pairs acquired with each configuration. Differences in T_2 relaxation time measurements between dual-coil-array and single-coil-array acquisitions were compared to the standard repeatability of single-coil-array measurements using a Bland-Altman analysis.

Results—Mean g-factors for the dual-coil-array configuration were low for accelerations up to 6 in the right-left direction and minimal cross-talk is observed between the two coil-arrays. Image quality ratings of various joint tissues showed no difference in 89%(95% CI:85–93%) of rated image pairs with only small differences (“slightly better” or “slightly worse”) in image quality observed. T_2 relaxation time measurements between the dual-coil-array configuration and the single-coil configuration showed similar limits of agreement and concordance correlation coefficients [limits of agreement: −0.93-1.99 ms; CCC:0.97(95% CI:0.96-0.98)], to the repeatability of single-coil-array measurements [limits of agreement: −2.07-1.96 ms; CCC: 0.97(95% CI: 0.95-0.98)].

Conclusion—A bilateral coil-array setup can image both knees simultaneous in similar scan times as conventional unilateral knee scans with comparable image quality and quantitative accuracy. This has the potential to improve the value of MRI knee evaluations.

Keywords

Knee MRI; Osteoarthritis; Parallel Imaging; T2 Mapping

Corresponding Author: Feliks Kogan, PhD, Stanford University, Department of Radiology, 1201 Welch Rd, Stanford, CA 94305, fkogan@stanford.edu, 585.733.8684.

INTRODUCTION

Osteoarthritis (OA) remains a tremendous burden to society, affecting the majority of the population by age 65[1]. Not only is OA a leading cause of pain and disability, it also has alarge economic burden, costing the US economy anestimated 185 billion dollars per year[2,3]. Despite its prevalence and large socioeconomic costs, OA remains a poorly understood disease and the only definitive treatment for knee OA is total joint replacement, an invasive and expensive surgery with known long term complications[4]. Magnetic resonance imaging (MRI) is a promising tool to non-invasively study the complex disease processes involved in knee OA[5,6]. MRI can provide high-resolution morphologic information of the knee with multiple different contrasts. Additionally, advanced quantitative MRI techniques, such as T_2 and $T_{1\rho}$ relaxation time mapping, can provide tissue biochemical information about collagen matrix organization, glycosaminoglycan (GAG) content, and hydration[7–10].

OA is commonly a bilateral disease[11]. While long scan time and costs have precluded separate scanning of both knees in clinical MRI, there is evidence that bilateral examinations are beneficial for evaluation of OA changes, especially for longitudinal studies[12]. The Osteoarthritis Initiative (OAI), a 4800 patient longitudinal multi-center study of OA study costing over $100 million sponsored by the NIH, included MRI on both knees to increase statistical power and correlate with other findings[13]. Other studies commonly use the contralateral knee for comparison, particularly if there is an injury to one knee, such as tears to the meniscus or anterior cruciate ligament[14]. Unfortunately, even when both knees are studied, scan time restrictions and costs often limit the MRI protocol. The OAI used a 1-hour MRI protocol to minimize patient motion and withdrawals from the study. This limited MRI to primarily morphologic evaluation, allowing only a single physiologic study (T_2 mapping) in only one knee. Simultaneous imaging of both knees without added scan time can drastically reduce scan costs, improve patient comfort and retention, and eliminate potential parameter/sequence differences between scans of each knee.

Optimized simultaneous MR imaging of both knees is feasible through utilization of two coil-arrays around each knee. While methods for bilateral imaging have received limited attention for knee imaging, numerous methods have been developed for optimized bilateral breast imaging[15,16], a similar problem. If two coil-arrays are “independent”, meaning there is no coupling of coil elements between the two coil-arrays, then both knee volumes can be imaged without affecting image signal-to-noise ratio (SNR) compared to single knee scans, by simply exciting and encoding both sides. For 2D axial or coronal acquisitions, excitation is unchanged while for 3D acquisitions, the volume can just be expanded to include both knees. For encoding, if phase-encoding is in the left/right direction, parallel imaging techniques can be utilized[17]. On the other hand, if left/right is a readout direction, the bandwidth and matrix can be increased together. Lastly, in the case that left/right is the slice direction for a 2D acquisition, a multiband excitation would be needed in combination with simultaneous multi-slice (SMS) encoding[18].

In this work, we describe a bilateral coil setup using two 16-channel flexible coil-arrays to scan both knees simultaneously with similar scan time, image quality, and quantitative accuracy compared to single knee acquisitions. We evaluate noise covariance maps to understand coupling of coil elements, sensitivity encoding (SENSE)[19] g-factor maps to assess parallel imaging noise amplification. Finally we compare image quality in morphologic sequences as well as quantitative values in a T_2-mapping sequence between unilateral knee and bilateral knee acquisitions of similar scan times.

METHODS

All imaging experiments were performed on a 3.0T GE MR750 scanner (GE Healthcare, Milwaukee, WI). MR imaging was performed with two 16-channel flexible phased-array, receive only, medium sized extremity coils (NeoCoil, Pewaukee, WI). Due to restrictions on having 2 coils with the same coil ID connected at the same time on the scanner, one coil was modified by replacing the resistor that effectively selects the coil ID and creating a new coil configuration file on the scanner to enable using both coils at once. Safety testing was then performed by running the scanner with a spoiled gradient echo (SPGR) sequence at the maximum allowable specific absorption rate (SAR) for one hour to ensure no additional heating was observed in the dual-coil configuration. Figure 1 shows the patient in the supine position with the two coil-arrays around each knee separated by a thin foam pad. Prior to participating in the study, all subjects were informed about the nature of the study and provided informed consent according to the University Institutional Review Board. The study was Health Insurance Portability and Accountability Act (HIPAA) – compliant.

Dual-Coil-Array Performance

One volunteer was imaged to determine the noise covariance and parallel imaging geometry factors (g-factors) of the dual-coil-array configuration. The noise covariance matrix describes the Gaussian noise and coupling of coil elements while the g-factor reflects the coil array's ability to unfold aliased images under subsampling. Noise-only data (with no radiofrequency pulse) was acquired using the dual-coil-array configuration, and the noise covariance matrix (Ψ) was estimated using Eq. 1,

$$\Psi_{ij} = (1/N) \sum_{k=1}^{N} r_i^*(k) r_j(k) \quad [1]$$

where $r_{i,j}(k)$ is the complex signal value from coil i and j, respectively, in k-space location k and N is the number of noise samples acquired. Coil sensitivities were estimated from fully-sampled data using the ESPIRiT method and a 24×24 calibration region[20]. ESPIRiT provides accurate coil sensitivity map estimates that are cropped to exclude regions far outside of the anatomy and have an otherwise homogeneous scaling. Images were retrospectively subsampled and reconstructed and g-factor maps were computed using SENSE analytical expressions including the estimated noise covariance[19]. Acceleration factors in the phase (R_y) and slice (R_z) directions of 1×2, 1×3, 1×4, 1×5, 1×6 and 2×2, respectively were evaluated.

Additionally, one volunteered was imaged to evaluate the effect of shimming over both knees in the dual-coil-array configuration. After performing an automatic shim across a volume including both knees, a spectral scan was used to determine the water line width, measured as the full-width at half maximum (FWHM) of the water spectral peak. For comparison, this measurement was repeated with a single knee in the single-coil-array configuration.

MRI Scanning

10 healthy subjects were recruited for this study. The dual-coil-array configuration was used to scan both knees first. The coil-array on the left knee was then removed and the right knee was scanned in a conventional single-coil-array configuration. The imaging protocol included 2D coronal and axial proton density (PD) weighted fat-suppressed (FS) fast-spin echo (FSE) acquisitions as well as a 3D sagittal quantitative double-echo in steady-state (DESS) sequence[21]. 2D coronal FSE and 3D sagittal DESS sequences used parallel imaging acceleration with ARC (Autocalibrating Reconstruction for Cartesian imaging) to undersample in the right-left direction for bilateral knee scans in order to maintain similar scan times compared to single knee acquisitions. For bilateral 2D axial FSE scans, the frequency direction was set to right-left and the field-of-view (FOV) was extended in the readout direction to maintain similar scan times. The bandwidth per pixel was maintained between unilateral and bilateral knee acquisitions. Scan parameters are listed in Table 1. The DESS scan was performed twice with the single-coil-array configuration to evaluate variation in T_2 relaxation time measurements.

Image and Statistical analysis

For comparison, bilateral knee acquisition images were cropped to have the same FOV in all three dimensions as single knee acquisitions. Two experienced musculoskeletal radiologists with 23 (G.G) and 13 (E.O.) years of experience, respectively, compared relative image quality between images acquired with single and dual-coil configurations. Images were presented as pairs and the radiologists were blinded to which image set was acquired with which configuration. The radiologists evaluated [1] Cartilage, [2] Meniscus, [3] Tendons/Ligaments, [4] Bone/Bone Marrow/Fat features for each sequence across the 10 subjects. A five-point scale was used to comparatively score single-coil and dual-coil images, which were blinded and randomized:

−2 - Image 01 much worse than Image 02

−1 - Image 01 slightly worse than Image 02

0 - No difference

+1 - Image 01 slightly better than Image 02

+2 - Image 01 much better than Image 02

Systematic disagreement between reader ratings was tested by an exact test of symmetry.

T_2 relaxation times were determined for articular cartilage using Extended Phase Graph (EPG) modeling of the relationship between the two DESS signals as previously described[8].

One experienced researcher (F.K.) segmented 3 slices in each of the medial, central and lateral sections of each knee into 8 cartilage compartments (Patella, Trochlea, Central and Posterior Medial Femoral Condyle, Central and Posterior Lateral Femoral Condyle and Medial and Lateral Tibia). The mean T_2 relaxation time across the sampled slices in each cartilage compartment was measured for the three acquired DESS datasets. Repeatability of T_2 measurements between dual-coil-array and single-coil-array acquisitions as well as for single-coil-array acquisitions was assessed by the Bland-Altman method and calculation of the concordance correlation.

RESULTS

Dual-Coil-Array Performance

The noise correlation matrix for the 32 channels in the dual-coil-array configuration shows little cross-talk between the two coil-arrays (channel numbers 1-16 vs 17-32) (Fig. 2). Channel 24 (Channel 8 in the second coil-array) was found to be receiving minimal power, which resulted in the low signal observed in that channel. Figure 3 shows the SENSE g-factor maps for an axial slice through both knees of a healthy volunteer. The g-factors maps were symmetric across both coil-arrays for all acceleration factors tested. Mean g-factors ranged from 1.00 for an acceleration factor, R_z=2, to 1.38 for an acceleration factor R_z=6. Sagittal images of the first echo of the DESS sequence acquired with the dual-coil-array configuration and reconstructed with various subsampling factors show similar image quality (Fig. 4). Lastly, an increase of 15 Hz in the water linewidth was observed when shimming and scanning across both knees in the dual-coil-array configuration (FWHM = 61 Hz) compared to conventional single knee scans (FWHM = 46 Hz).

Dual-Coil-Array Image Quality

Figures 5 and 6 show acquired bilateral knee scans with the dual-coil-array configuration as well as dual-coil-array and single-coil-array images of the same FOV for axial and coronal 2D PD-weighted FSE scans, respectively, in a healthy volunteer. Sagittal images of the two DESS echo images show similar image quality between single-coil-array (Figs. 7a,7c) and dual-coil-array acquisitions (Figs. 7b,7d).

Image quality ratings of various joint tissues by two blinded reviewers showed mainly no difference between single-coil-array and dual-coil-array acquisitions (Table 2). Overall, 89% of the ratings were “0” or no difference between the image pairs (95% Confidence Interval (CI): 85-93%). There were no ratings of “2” or “−2” (much better or much worse), suggesting no substantial differences between the images from the two acquisitions. There was a marginal tendency for Reader 1 to rate images from the dual-coil-array configuration as slightly worse (“−1” instead of “0”) than Reader 2 (symmetry test p = 0.030). Reader 1 also noted that he “found image quality very similar between the two scans and cannot completely rule out some subjectivity, or some “differences” being attributable to partial volume.” Reader 1 rated dual-coil-array images as slightly worse image quality for axial PD FSE scans in cartilage in 6 of 10 cases and bone in 4 of 10 cases. All other scans and joint tissues were rated as “0” (no difference) at least 80% of the time by each reader and sagittal

DESS acquisitions were rated to produce equivalent image quality between the two acquisitions by both readers for all tissues in all cases.

Dual-Coil-Array Quantitative Accuracy

Bilateral knee MRI acquisitions with the dual-coil-array configuration also maintained quantitative accuracy of measured T_2 relaxation times compared with single-knee, single-coil-array acquisitions. Figures 7e,7f demonstrate representative T_2 relaxation time maps of acquired with single-coil-array and dual-coil-array configurations, respectively. The mean difference in T_2 relaxation time measurements between the dual-coil-array configuration and the single-coil-array configuration was 0.53±0.74 ms (95% limits of agreement: −0.93 - 1.99 ms) with a concordance correlation coefficient of 0.97 (95% CI: 0.96-0.98) (Fig. 8a). This was similar to the repeatability of the single-coil-array T_2 relaxation time measurements for which a mean difference of −0.06±1.03 ms (95% limits of agreement: −2.07 - 1.96 ms) with a concordance correlation coefficient of 0.97 (95% CI: 0.95-0.98) (Fig. 8b) was observed.

DISCUSSION

This work has shown that a bilateral coil-array setup can image both knees simultaneously in similar scan times to conventional unilateral knee scans, while maintaining image quality and quantitative accuracy.

Coil-array performance testing demonstrated the potential to use the dual-coil-array configuration in combination with parallel imaging to scan both knees simultaneously in roughly the same scan time with minimal loss of image quality. The noise covariance matrix showed that the two coil-arrays were largely decoupled from one another. Similarly, for SENSE reconstructions, mean g-factors were low (below 1.4 for an R_Z up to 6) for the dual-coil-array configuration. g-factor is a measure of a coil array's ability to unfold under-sampled accelerated images. It is directly related to SNR, which is inversely proportional to the g-factor as well as the square root of the acceleration factor, R. For 3D sagittal DESS images, an acceleration factor of three (R_Z=3) was used in the slice (right-left) direction. While the data was under-sampled by a factor of 3, this was offset by 3 times more phase encodes in the z-direction (120 slices for bilateral knee scans vs 40 slices in the single knee scans). Thus, due to the low g-factor of the dual-coil-array configuration for R_Z=3 (mean g-factor =1.01), this resulted in a negligible change in image SNR compared to fully-sampled single knee acquisitions, with only a 6 second increase in scan time to acquire the ARC calibration region. Similarly, for 2D coronal FSE scans, the doubling of number of phase encodes in the y direction (right-left) offset the acceleration in the same direction resulting a minimal loss of SNR due to coil-array g-factor (mean g-factor=1.00).

Different acquisition and parallel imaging methods can be utilized to take advantage of the dual-coil setup to scan both knees simultaneously. As mentioned above, our 3D sagittal DESS and 2D coronal FSE scans utilized parallel-imaging acceleration in right-left direction. This strategy is available for Cartesian acquisitions in all three scan planes for 3D acquisitions as well as for coronal and axial planes for 2D acquisitions. For axial Cartesian acquisitions, it is also possible to acquire frequency information in the right-left direction allowing both knees to be scanned without acceleration in a similar scan time to single knee

scans, as we showed in the 2D axial FSE images. One potential drawback of this approach is that flow artifacts from the popliteal artery appear in phase direction, which becomes anterior-posterior (for an R-L frequency direction) rather than the traditional right-left direction (for an A-P frequency direction), which may affect diagnostic quality. Nevertheless, if this is an issue, an acceleration approach similar to the 2D coronal FSE scans can of course be utilized allowing the frequency direction to remain unchanged.

Similar image quality was observed between dual-coil-array and single-coil-array images, as evaluated by blinded pairwise comparison of images from the two configurations by experienced radiologists. Only small differences (slightly better or slightly worse) in image quality were observed in the few image pairs which were not graded as “no difference” and the majority of those were in the axial images where flow artifacts from the popliteal artery may have been an issue. As mentioned above, clinical scans can maintain their preferred phase direction and utilize undersampling acceleration methods if this is an issue.

Bilateral knee T_2 relaxation time mapping with the dual-coil-array approach showed similar quantitative T_2 values compared to single-knee acquisitions with a single coil-array. The limits of agreement and concordance correlations in measurements of T_2 between the dual-coil-array configuration and a traditional single-coil-array configuration were comparable to that of the repeatability of single-coil-array measurements. It is important to note that quantification of T_2 relaxation time values still varies between different pulse sequences[22]. However, this data suggests that utilizing the dual-coil-array approach to image both knees simultaneously has minimal effect on these measurements.

Simultaneous bilateral knee MRI offers opportunities to improve the value of knee MRI in both clinical and research settings. For clinical exams, information regarding the contralateral knee may serve as an internal control for clinical evaluation of anatomy, joint injury, or sources of pain. In research exams, this can be expanded to provide an internal control of quantitative MRI values. In research studies which require scanning of both knees, bilateral knee MRI can drastically reduce scan costs, reduce patient motion, improve patient retention, and eliminate potential sources of error between scans of each knee. Finally, fast bilateral MRI can further help the clinical value of PET/MR knee imaging as PET data is already acquired simultaneously from both knees and scan time is limited by MRI acquisition time[23,24].

Scanning of both knees simultaneously also has a few challenges. First, it is not possible to utilize parallel imaging in the right-left direction for conventional 2D sagittal Cartesian acquisitions. Nevertheless, those sequences could be scanned on each knee separately, or in an interleaved-slice approach. This set-up would still be beneficial compared to repositioning the coil and repeating the protocol. Additionally, new imaging methods using simultaneous multi-slice (SMS)[18] may offer a solution to this challenge. It is also not straightforward to accelerate sequences that utilize non-Cartesian k-space trajectories. For this, it may be possible to utilize optimized trajectories[25] and multiple demodulation hardware[26], along with the localized sensitivities of the individual coils[27]. Again, it is still possible to acquire each knee separately with those methods without coil repositioning. Another challenge is shimming over the larger field-of-view needed for scanning of both

knees. As evidenced by the increase in water linewidth when imaging across both knees, this may result in greater B_0 field inhomogeneity, which may affect image SNR as well as non inversion-recovery (IR) based fat-saturation methods. However, neither musculoskeletal radiologist noted this as a major concern as, at 3T and below, B_0 fields are relatively homogeneous. However, the may be a bigger concern for quantitative methods that are dependent on B_0 field homogeneity such chemical exchange saturation transfer (CEST) MRI.

It is important to note several limitations to this study. As previously mentioned, the phase-encode direction for axial PD-weighted FSE scans differed between single-coil-array and dual-coil-array acquisitions. This was done to demonstrate that the possibility of using a right-left frequency-encode direction to scan both knees with the same scan time as single-coil-array acquisitions without using parallel imaging. The flow artifacts across the knee that resulted from this may have led to some of the slight preferences in single-coil-array image quality for evaluation of bone marrow and cartilage that were observed with this sequence. It is also important to note that bilateral 3D DESS scans used an ARC reconstruction which may have affected quantitative measurements compared to the sum-of-squares (SoS) reconstruction used for single-knee acquisitions. However, measurements of T_2 relaxation times with bilateral acquisitions were still comparable to those of single-knee scans. Further, ARC reconstructed images may provide a more accurate measurement of T_2 values than those reconstructed with SoS since it accounts for coil sensitivities[28].

In summary, this work demonstrated the potential for simultaneous bilateral knee imaging using a dual-coil-array approach. It was shown that there was nominal cross-talk between each coil-array in the dual-coil-array configuration which created minimal coil noise amplification for dual-coil-array scans compared to single-coil-array scans. This allowed scanning of both knees simultaneously in similar scan times to single knee scans while maintaining image quality and quantitative accuracy. Simultaneous imaging of both knees can improve the value of MRI knee evaluations; providing an internal control for clinical evaluation of pathology as well as helping reduce costs and improve continuity in research studies.

Acknowledgments

We gratefully acknowledge Jorge Guzman for his expertise and help in MRI hardware and safety testing to allow simultaneous scanning with multiple flex coils. We would also like to thank Dr. Jarrett Rosenberg for all his with the statistical analysis. This work was funded by GE Healthcare and National Institute of Health (NIH) grants R01EB002524, R01AR0063643, K24AR062068 and K99EB022634.

LITERATURE CITED

1. Arden N, Nevitt MC. Osteoarthritis: epidemiology. Best Practice & Research Clinical Rheumatology. 2006; 20(1):3–25. [PubMed: 16483904]
2. Kotlarz H, Gunnarsson CL, Fang H, Rizzo JA. Insurer and out-of-pocket costs of osteoarthritis in the US: evidence from national survey data. Arthritis Rheum. 2009; 60(12):3546–3553. [PubMed: 19950287]
3. Hunter DJ, Schofield D, Callander E. The individual and socioeconomic impact of osteoarthritis. Nature reviews Rheumatology. 2014; 10(7):437–441. [PubMed: 24662640]

4. Weinstein AM, Rome BN, Reichmann WM, Collins JE, Burbine SA, Thornhill TS, Wright J, Katz JN, Losina E. Estimating the burden of total knee replacement in the United States. The Journal of bone and joint surgery American volume. 2013; 95(5):385–392. [PubMed: 23344005]
5. Matzat SJ, Kogan F, Fong GW, Gold GE. Imaging strategies for assessing cartilage composition in osteoarthritis. Current rheumatology reports. 2014; 16(11):462. [PubMed: 25218737]
6. Oei EH, van Tiel J, Robinson WH, Gold GE. Quantitative radiological imaging techniques for articular cartilage composition: Towards early diagnosis and development of disease-modifying therapeutics for osteoarthritis. Arthritis care & research. 2014
7. Liu F, Chaudhary R, Hurley SA, Munoz Del Rio A, Alexander AL, Samsonov A, Block WF, Kijowski R. Rapid multicomponent T2 analysis of the articular cartilage of the human knee joint at 3.0T. J Magn Reson Imaging. 2014; 39(5):1191–1197. [PubMed: 24115518]
8. Sveinsson B, Chaudhari AS, Gold GE, Hargreaves BA. A simple analytic method for estimating T2 in the knee from DESS. Magn Reson Imaging. 2017; 38:63–70. [PubMed: 28017730]
9. Singh A, Haris M, Cai K, Kogan F, Hariharan H, Reddy R. High resolution T1rho mapping of in vivo human knee cartilage at 7T. PloS one. 2014; 9(5):e97486. [PubMed: 24830386]
10. Kogan F, Hargreaves BA, Gold GE. Volumetric multislice gagCEST imaging of articular cartilage: Optimization and comparison with T1rho. Magn Reson Med. 2016
11. Metcalfe AJ, Andersson ML, Goodfellow R, Thorstensson CA. Is knee osteoarthritis a symmetrical disease? Analysis of a 12 year prospective cohort study. BMC musculoskeletal disorders. 2012; 13:153. [PubMed: 22917179]
12. Jungmann PM, Brucker PU, Baum T, Link TM, Foerschner F, Minzlaff P, Banke IJ, Saier T, Imhoff AB, Rummeny EJ, Bauer JS. Bilateral cartilage T2 mapping 9 years after Mega-OATS implantation at the knee: a quantitative 3T MRI study. Osteoarthritis Cartilage. 2015; 23(12): 2119–2128. [PubMed: 26115937]
13. Eckstein F, Kwoh CK, Link TM, investigators OAI. Imaging research results from the osteoarthritis initiative (OAI): a review and lessons learned 10 years after start of enrolment. Ann Rheum Dis. 2014; 73(7):1289–1300. [PubMed: 24728332]
14. Bae JH, Hosseini A, Wang Y, Torriani M, Gill TJ, Grodzinsky AJ, Li G. Articular cartilage of the knee 3 years after ACL reconstruction. A quantitative T2 relaxometry analysis of 10 knees. Acta Orthop. 2015; 86(5):605–610. [PubMed: 25854533]
15. Han M, Beatty PJ, Daniel BL, Hargreaves BA. Independent slab-phase modulation combined with parallel imaging in bilateral breast MRI. Magn Reson Med. 2009; 62(5):1221–1231. [PubMed: 19780156]
16. Nnewihe AN, Grafendorfer T, Daniel BL, Calderon P, Alley MT, Robb F, Hargreaves BA. Custom-fitted 16-channel bilateral breast coil for bidirectional parallel imaging. Magn Reson Med. 2011; 66(1):281–289. [PubMed: 21287593]
17. Deshmane A, Gulani V, Griswold MA, Seiberlich N. Parallel MR imaging. J Magn Reson Imaging. 2012; 36(1):55–72. [PubMed: 22696125]
18. Barth M, Breuer F, Koopmans PJ, Norris DG, Poser BA. Simultaneous multislice (SMS) imaging techniques. Magn Reson Med. 2016; 75(1):63–81. [PubMed: 26308571]
19. Pruessmann KP, Weiger M, Scheidegger MB, Boesiger P. SENSE: sensitivity encoding for fast MRI. Magnetic Resonance in Medicine. 1999; 42(5):952–962. [PubMed: 10542355]
20. Uecker M, Lai P, Murphy MJ, Virtue P, Elad M, Pauly JM, Vasanawala SS, Lustig M. ESPIRiT–an eigenvalue approach to autocalibrating parallel MRI: where SENSE meets GRAPPA. Magn Reson Med. 2014; 71(3):990–1001. [PubMed: 23649942]
21. Staroswiecki E, Granlund KL, Alley MT, Gold GE, Hargreaves BA. Simultaneous estimation of T(2) and apparent diffusion coefficient in human articular cartilage in vivo with a modified three-dimensional double echo steady state (DESS) sequence at 3 T. Magn Reson Med. 2012; 67(4): 1086–1096. [PubMed: 22179942]
22. Matzat SJ, McWalter EJ, Kogan F, Chen W, Gold GE. T Relaxation time quantitation differs between pulse sequences in articular cartilage. J Magn Reson Imaging. 2014
23. Kogan F, Fan AP, McWalter EJ, Oei EHG, Quon A, Gold GE. PET/MRI of metabolic activity in osteoarthritis: A feasibility study. Journal of Magnetic Resonance Imaging. 2016:n/a–n/a.

24. Kogan F, Fan AP, Gold GE. Potential of PET-MRI for imaging of non-oncologic musculoskeletal disease. Quantitative Imaging in Medicine and Surgery. 2016; 6(6):756–771. [PubMed: 28090451]

25. Addy NO, Ingle RR, Wu HH, Hu BS, Nishimura DG. High-resolution variable-density 3D cones coronary MRA. Magn Reson Med. 2015; 74(3):614–621. [PubMed: 26172829]

26. Lee JH, Scott GC, Pauly JM, Nishimura DG. Broadband multicoil imaging using multiple demodulation hardware: a feasibility study. Magn Reson Med. 2005; 54(3):669–676. [PubMed: 16086362]

27. Griswold MA, Jakob PM, Nittka M, Goldfarb JW, Haase A. Partially parallel imaging with localized sensitivities (PILS). Magn Reson Med. 2000; 44(4):602–609. [PubMed: 11025516]

28. Chaudhari AS, Sveinsson B, Moran CJ, McWalter EJ, Johnson EM, Zhang T, Gold GE, Hargreaves BA. Imaging and T2 relaxometry of short-T2 connective tissues in the knee using ultrashort echo-time double-echo steady-state (UTEDESS). Magn Reson Med. 2017

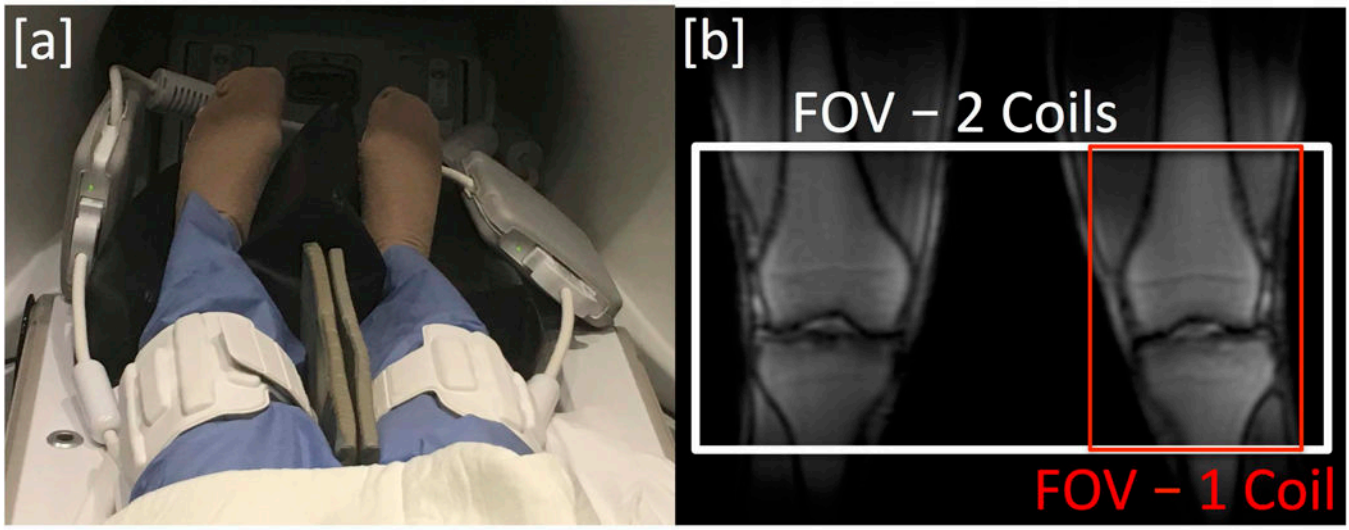

Figure 1.

[a] Dual-Coil-Array setup with two 16-channel flexible phased-array coils for bilateral knee imaging. [b] Sample localizer image and field-of-view for bilateral knee imaging with a dual-coil-array setup (120 slices – white) and single knee imaging with a single-coil-array setup (40 slices – red).

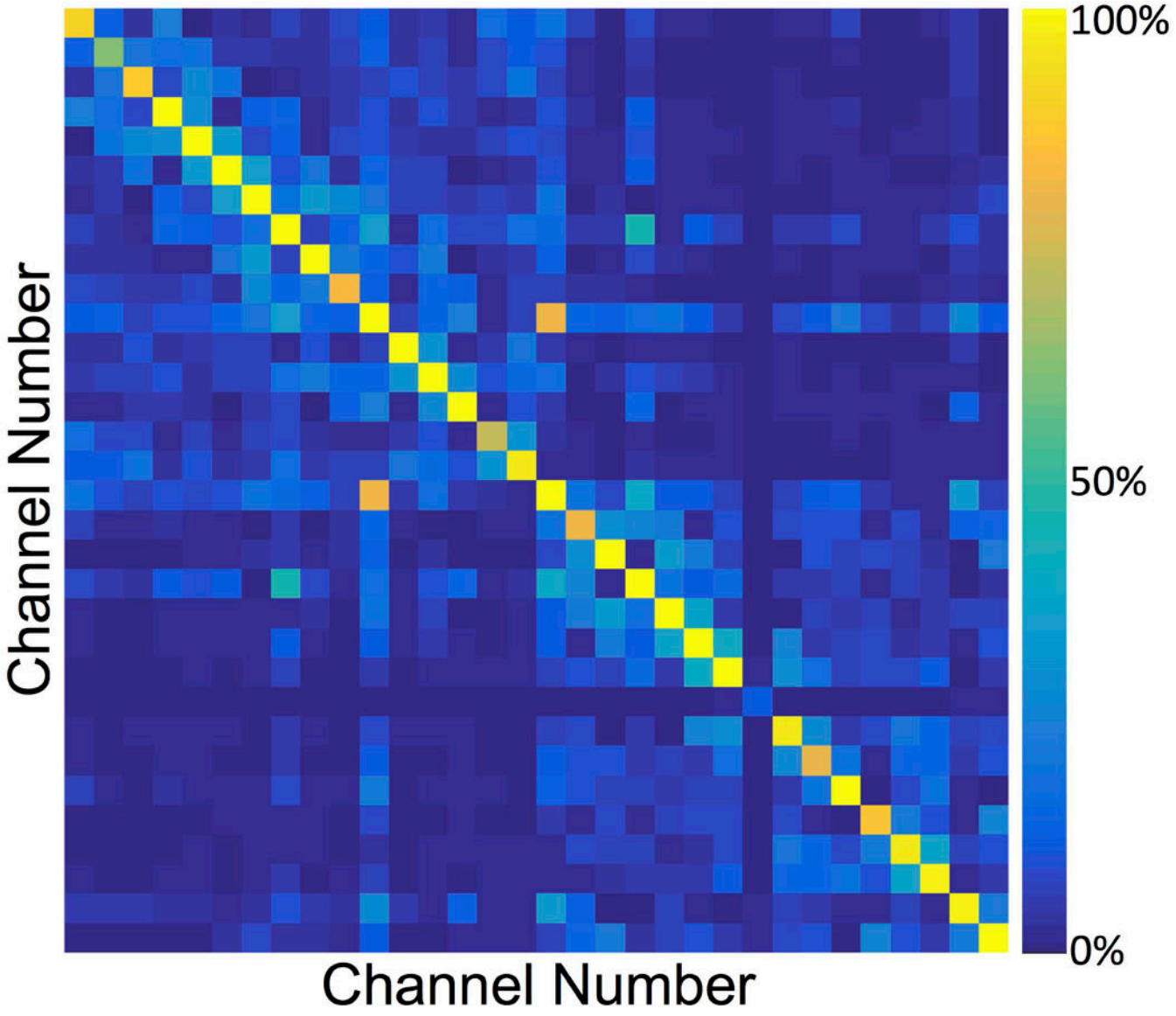

Figure 2.

Noise Correlation matrix from a healthy volunteer using the dual-coil-array configuration. [Note: Channel 24 (Channel 8 in the second coil-array) was found to be a dead element (receiving minimal power), which resulted in the low signal observed in that channel].

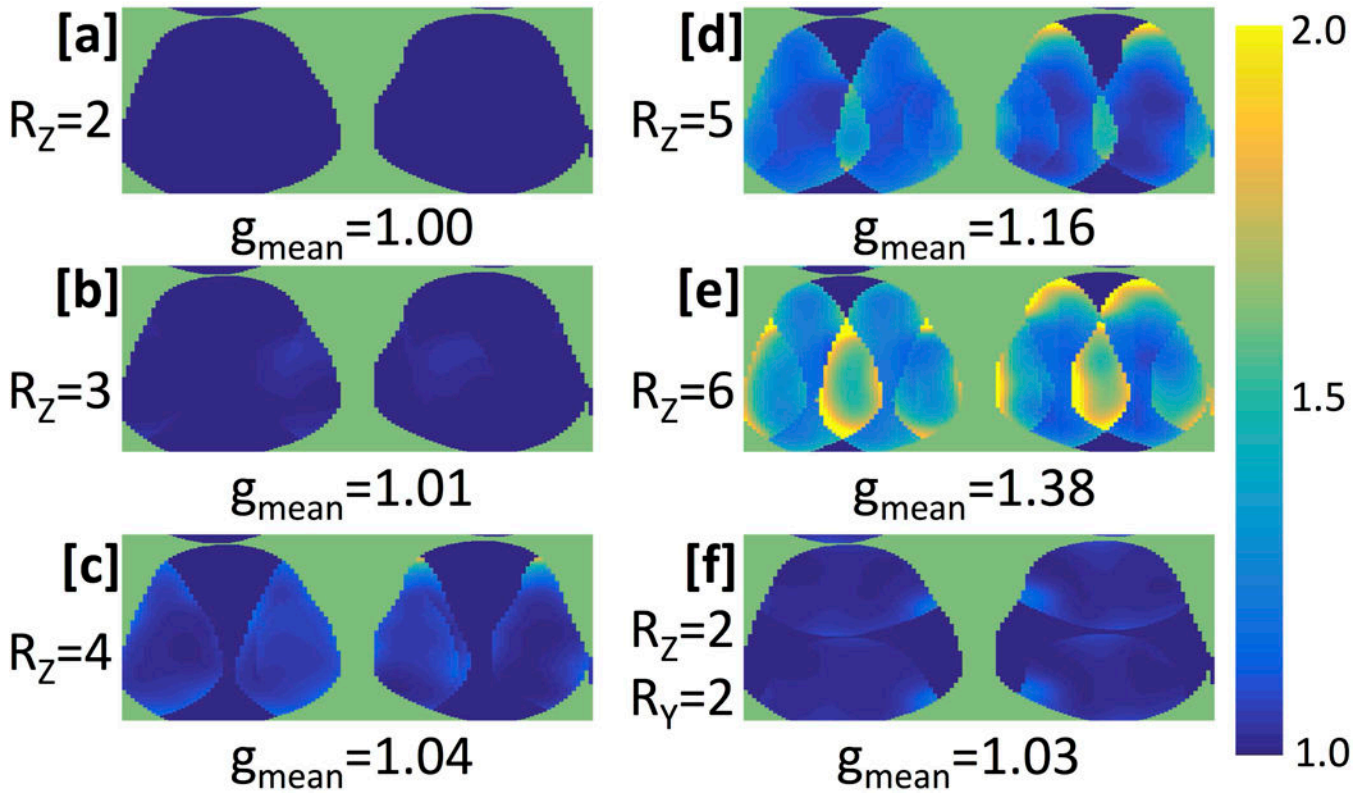

Figure 3.

SENSE g-factor maps and mean g-factor values of an axial slice of both knees of a healthy volunteer. Full k-space data was acquired with a 3D DESS scan which was retrospectively subsampled in the R_y (a/p) and R_z (l/r) directions, respectively by [a] 1×2, [b] 1×3, [c] 1×4, [d] 1×5, [e] 1×6 and [f] 2×2.

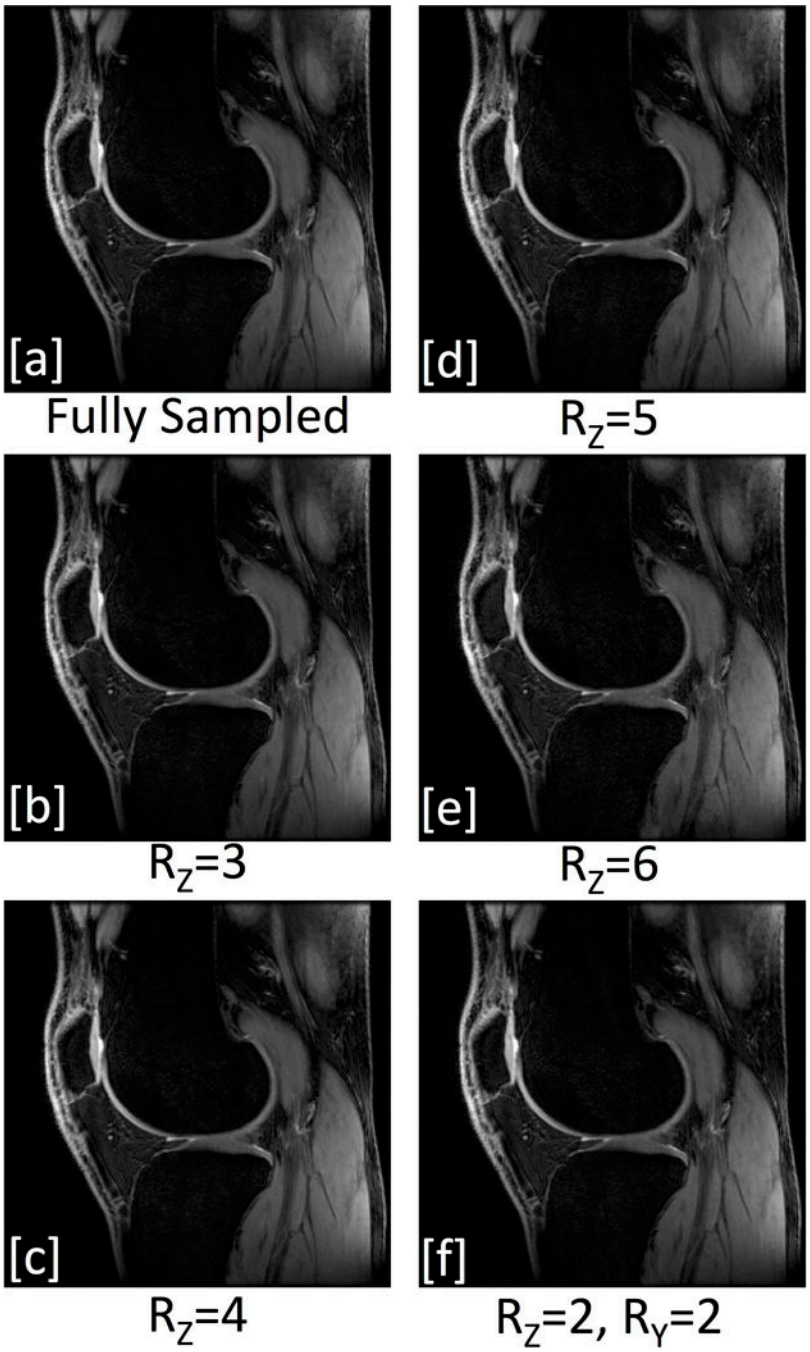

Figure 4.

Sagittal DESS first-echo (TE= 5.1 ms) image acquired with the dual-coil-array configuration and reconstructed with [a] full k-space data as well as data k-space retrospectively subsampled in the R_y (a/p) and R_z (l/r) directions, respectively by [b] 1×3, [c] 1×4, [d] 1×5, [e] 1×6 and [f] 2×2. [Images scaled to maximum pixel intensities].

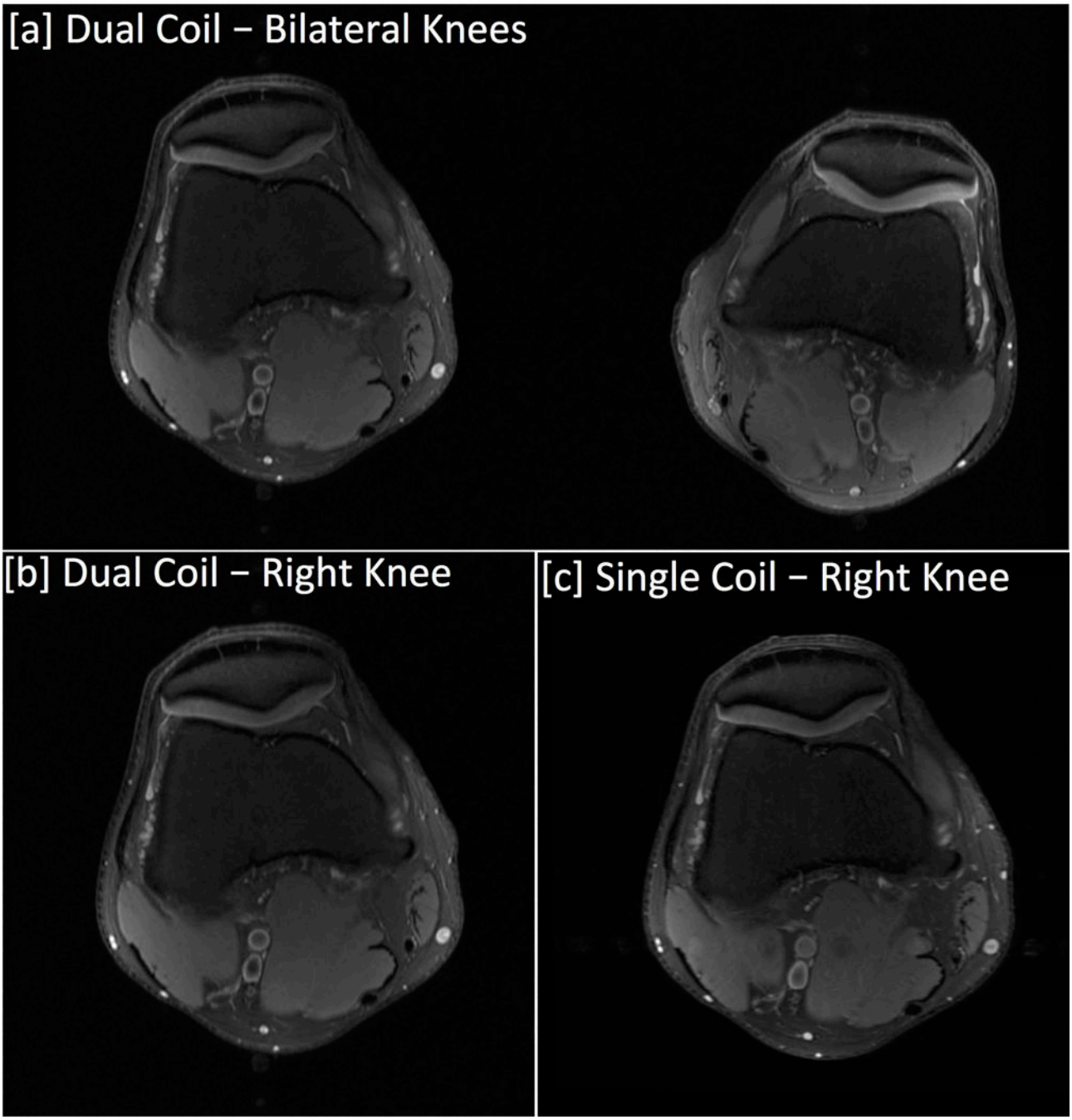

Figure 5.

Axial PD-weighted Fat Suppressed FSE images acquired with dual-coil-array and single-coil-array configurations. [a] Bilateral knee images acquired with the dual-coil-array configuration. [b] The bilateral knee image cropped to have the same FOV for comparison with the single knee image acquired with a traditional single-coil-array configuration. The frequency direction for bilateral scans was applied in the right-left direction to maintain scan time compared to single knee acquisitions.

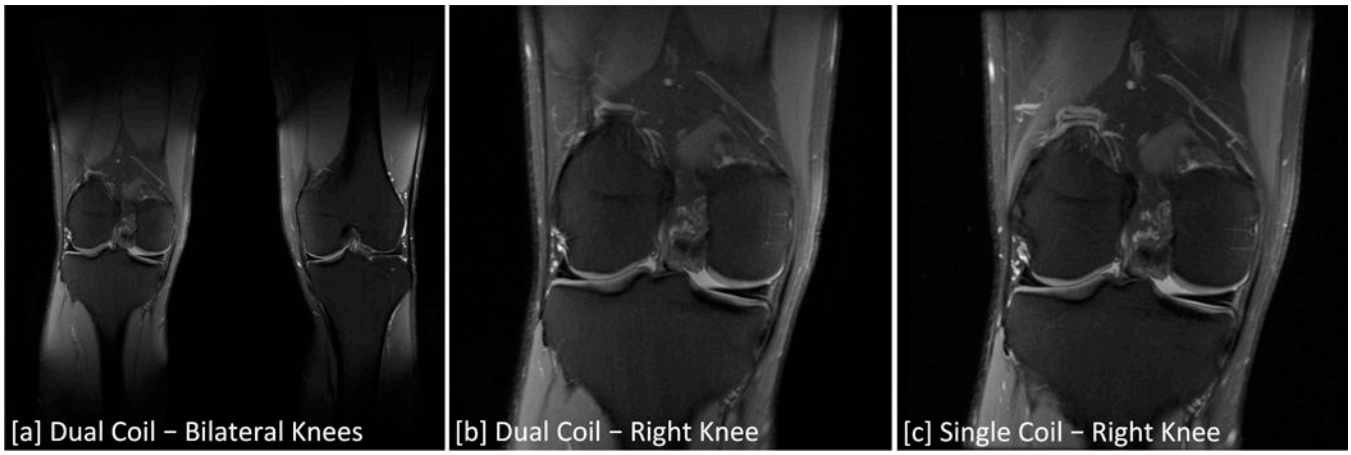

Figure 6.

Coronal PD-weighted Fat Suppressed FSE images acquired with dual-coil-array and single-coil-array configurations. [a] Bilateral knee images acquired with the dual-coil-array configuration. [b] The bilateral knee image cropped to have the same FOV for comparison with the single knee image acquired with a traditional single-coil-array configuration. Bilateral scans used a larger FOV and undersampling in the phase (right-left) direction to image both simultaneously in similar scan times to single knee acquisitions.

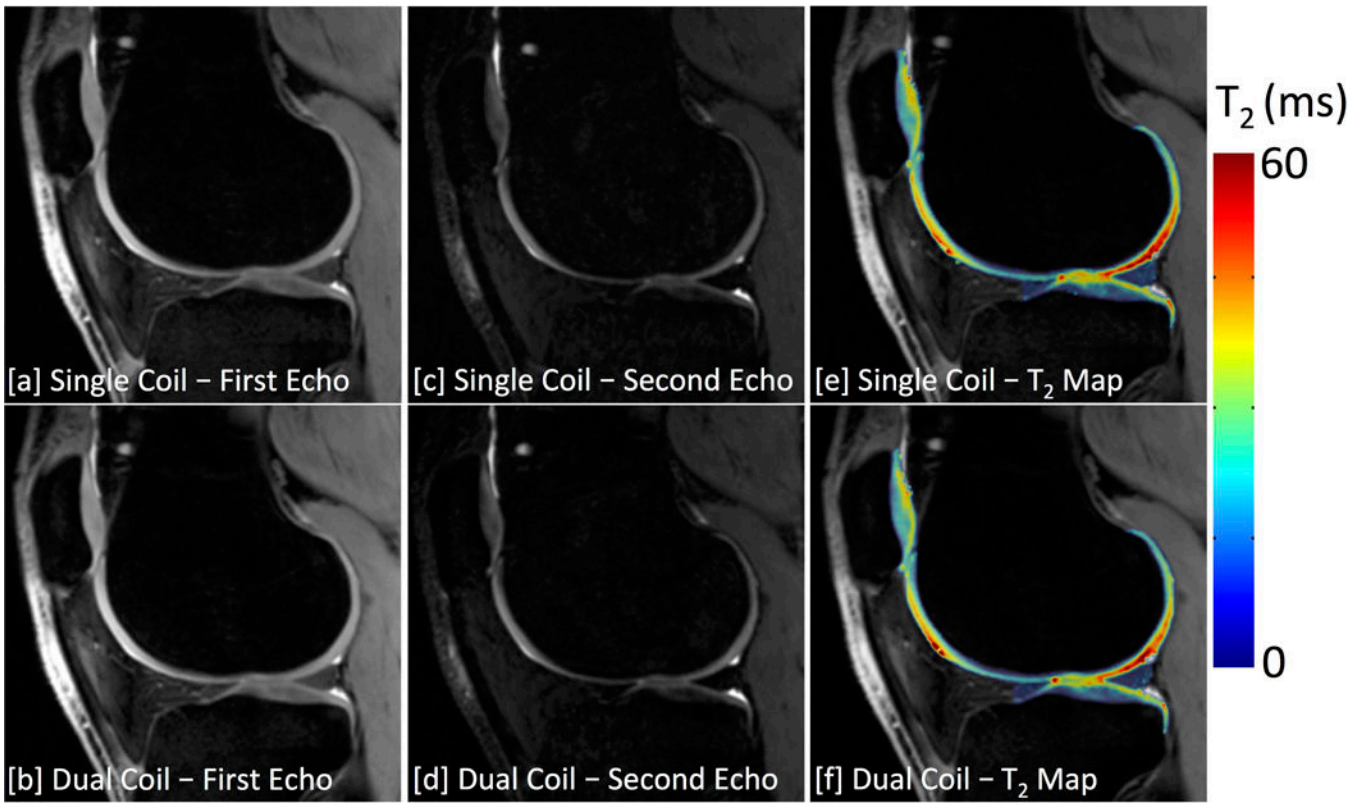

Figure 7.

3D DESS images of the [a,b] first echo, [c,d] second echo, and [e,f] the computed T_2 relaxation time maps acquired using a single-coil [top row] and dual-coil [bottom row] configurations. Bilateral scans used a factor of 3 undersampling in the slice-encode (right-left) direction to acquire images of both knees simultaneously in similar scan times to traditional single-knee acquisitions.

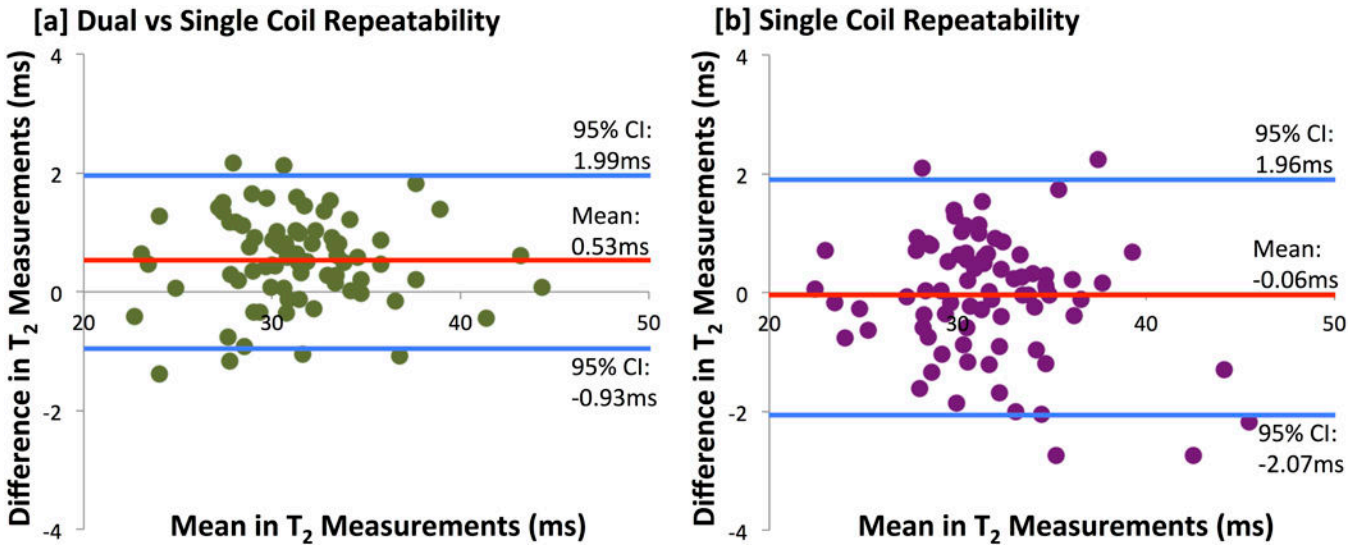

Figure 8.

Bland-Altman plot of the difference in T_2 measurements in 8 knee compartments across 10 subjects between [a] dual-coil-array configuration and the single-coil-array configuration as well as for the [b] repeatability of single-coil-array measurements.

Table 1

Scan parameters of MR imaging in single coil-array and dual coil-array configurations

	3D Double Echo Steady State		2D Coronal PD-Weighted FSE		2D Axial PD-Weighted FSE	
	Single Coil	**Dual Coil**	**Single Coil**	**Dual Coil**	**Single Coil**	**Dual Coil**
Scan Plane	Sagittal		Coronal		Axial	
FOV	16.0 cm		16.0 cm	35.0 cm	16.0 cm	35.0 cm
% Phase FOV	100	100	100	100	100	50
Matrix	256 × 256		352 × 224	768 × 448	352 × 224	768 × 448
Slice Thickness	3.0 mm		3.0 mm		3.0 mm	
$TR/TE_1/TE_2$	17.7/5.1/30.3 ms		3500/30 ms		3500/30 ms	
Slices	40	120	32	32	32	32
Frequency Direction	Anterior/Posterior		Superior/Inferior		Anterior/Posterior	Right/Left
Echo-train length	–	–	8	8	8	8
Fat Saturation	Water Selective		Chemical Saturation		Chemical Saturation	
Acceleration *	–	3 × 1	–	2 × 1	–	–
Scan Time	3:01	3:07	3:23	3:51	3:23	3:23

* Parallel imaging acceleration with ARC (Autocalibrating Reconstruction for Cartesian imaging) in the right-left direction

Table 2

Differences in image quality ratings between single-coil-array and dual-coil-array acquisitions from two blinded readers (No ratings of +2 or −2 were observed)

Cartilage										
		Sequence and Reader 2 Rating								
		Axial PD FSE			**Coronal PD FSE**			**Sagittal DESS**		
		−1	**0**	**+1**	**−1**	**0**	**+1**	**−1**	**0**	**+1**
Reader 1 Rating	**−1**	1	5	0	1	2	0	0	0	0
	0	0	4	0	0	6	1	0	10	0
	+1	0	0	0	0	0	0	0	0	0
Meniscus										
		Sequence and Reader 2 Rating								
		Axial PD FSE			**Coronal PD FSE**			**Sagittal DESS**		
		−1	**0**	**+1**	**−1**	**0**	**+1**	**−1**	**0**	**+1**
Reader 1 Rating	**−1**	0	0	0	0	0	0	0	0	0
	0	0	10	0	0	10	0	0	10	0
	+1	0	0	0	0	0	0	0	0	0
Tendons										
		Sequence and Reader 2 Rating								
		Axial PD FSE			**Coronal PD FSE**			**Sagittal DESS**		
		−1	**0**	**+1**	**−1**	**0**	**+1**	**−1**	**0**	**+1**
Reader 1 Rating	**−1**	0	0	0	0	0	0	0	0	0
	0	0	8	0	1	8	1	0	10	0
	+1	0	2	0	0	0	0	0	0	0
Bone/Bone Marrow/Fat										
		Sequence and Reader 2 Rating								
		Axial PD FSE			**Coronal PD FSE**			**Sagittal DESS**		

Cartilage

		Sequence and Reader 2 Rating								
		Axial PD FSE			Coronal PD FSE			Sagittal DESS		
		−1	0	+1	−1	0	+1	−1	0	+1
Reader 1 Rating	−1	0	4	0	0	2	0	0	0	0
	0	0	6	0	1	6	1	0	10	0
	+1	0	0	0	0	0	0	0	0	0

−1 - Dual Coil Images slightly worse than Single Coil Images

0 - No Difference between Images

+1 - Dual Coil Images slightly better than Single Coil Images